Challenges in coupled-channels calculations

Henning Esbensen
Argonne National Laboratory, Argonne, Illinois.

INT, October 24, 2013.

- The goal is to develop a coupled-channels description that explains
  - the enhancement of fusion at sub-barrier energies,
  - the hindrance at extreme sub-barrier energies,
  - and the suppression of data far above the Coulomb barrier.

- The basic description should include couplings to the low-lying 2^+ and 3^- states, two-phonon & mutual excitations of these states. It should rely on a predictable ion-ion potential. One should also consider the influence of multi-phonon excitations and transfer.

Work supported by U.S. Department of Energy,
Office of Nuclear Physics

Argonne NATIONAL LABORATORY

Short History of Heavy-ion Fusion.

- In the 1970s fusion was measured mostly at energies above the Coulomb barrier. *Surpass the barrier and the system is trapped!*
- In the 1980s cross sections were measured down to 0.1 mb.
  A large enhancement was observed at sub-barrier energies.
  Coupled-channels calculations were developed. *Calculated cross sections are strongly influenced by couplings at the Coulomb barrier! Fusion occurs once the barrier has been penetrated.*
- In the 1990s fusion data were measured with high precision.
  That allowed a better insight into the finer details of fusion.
- New challenges were recognized in the 2000s:
  - a strong hindrance was observed at very low energies (ANL),
  - a suppression of the data was observed at high energies (ANU).
  What causes these phenomena?

Conventional coupled-channels calculations

explain data near the Coulomb barrier: $0.1 < \sigma_f < 200$ mb,

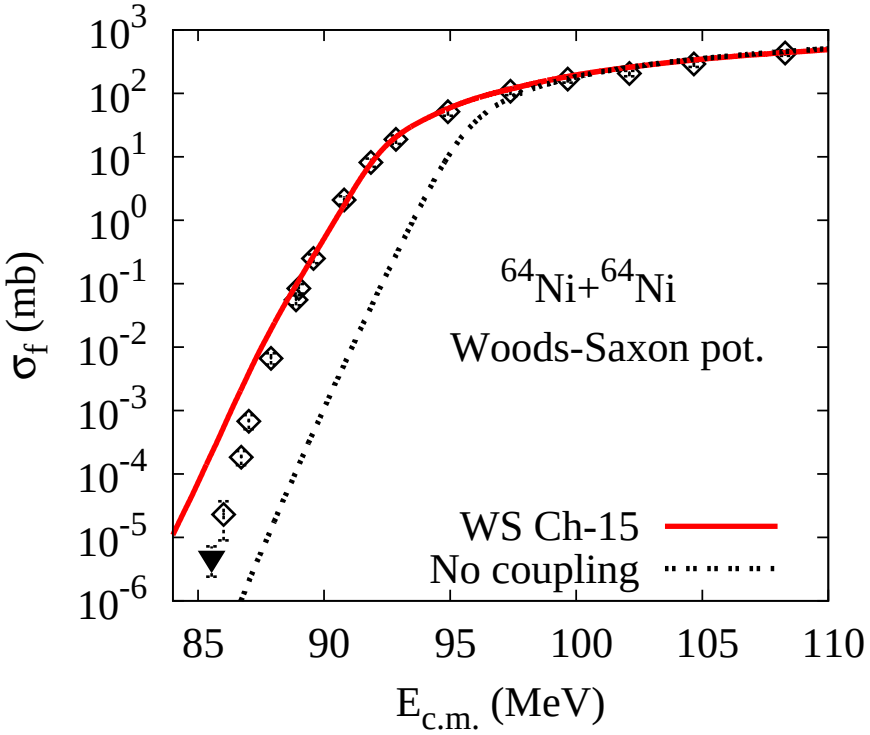

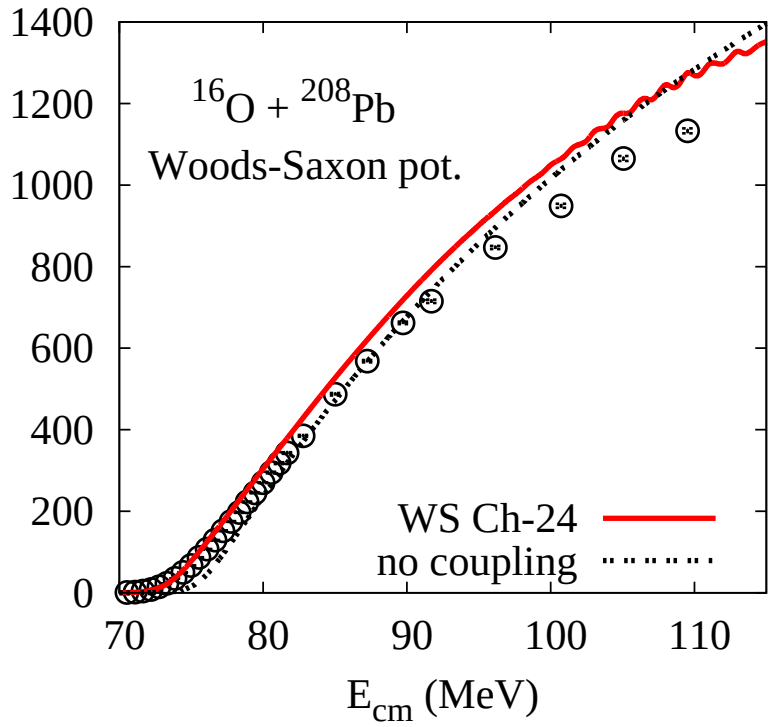

but not always **far below** or **far above** the Coulomb barrier.

^{64}Ni+^{64}Ni: V_{CB} = 95.2 MeV, ^{16}O+^{208}Pb: V_{CB} = 75.6 MeV.

^{64}Ni+^{64}Ni data by *Jiang et al.*, PRL 93, 012701 (2004).

^{16}O+^{208}Pb data by *Morton et al.*, PRC 60, 044608 (1999).

Basic assumptions in coupled-channels description.

- *Fusion can be simulated by ingoing-wave boundary conditions* (*IWBC*) that are imposed at the minimum of the *potential pocket.*

Coulomb barrier and pocket in the entrance channel potential:

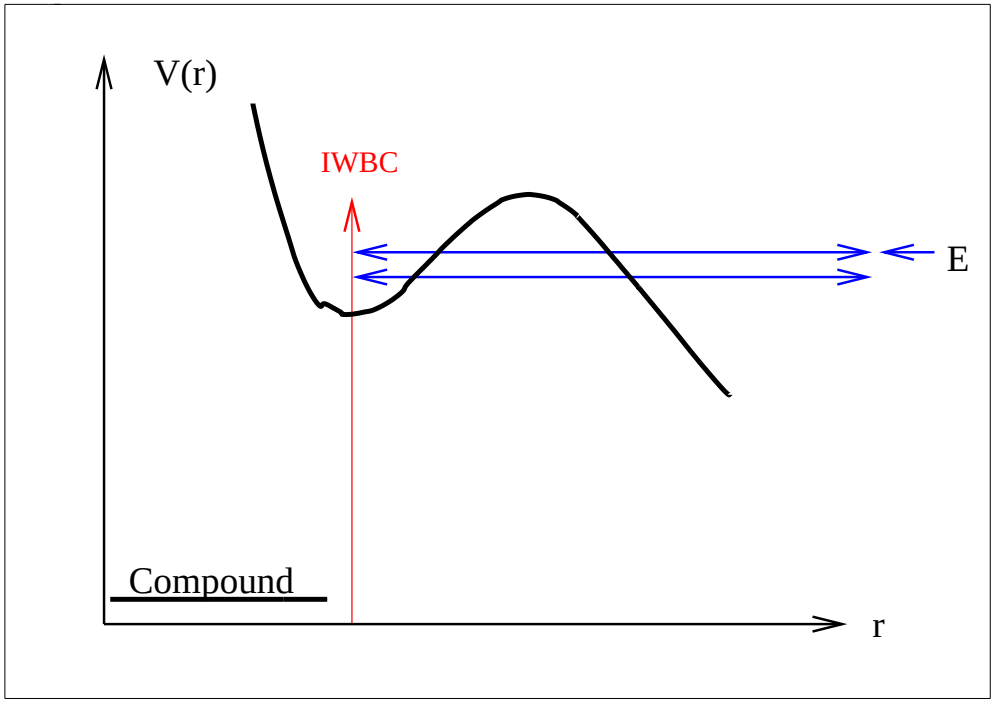

IWBC are sometimes supplemented with a weak, short-ranged imaginary potential.

- *Structure properties of nuclei do not change during the reaction.*
- *Excitation and transfer are independent degrees of freedom.*

Standard approach to surface excitations.

Include Coulomb couplings δV_C to first order δR,

$$\delta R = \sum R\alpha_{\lambda\mu} Y^*_{\lambda\mu}(\hat{r}), \;\; \langle n\lambda|\delta R|0\rangle = \frac{\beta_{n\lambda} R}{\sqrt{4\pi}}.$$

Expand the nuclear interaction up to second order in δR,

$$\delta V_N = -U'(r)\,\delta R + \frac{1}{2}\,U''(r)\,\Big(\delta R^2 - \langle 0|\delta R^2|0\rangle\Big),$$

where $U(r)$ is the standard empirical Woods-Saxon potential,

$$U(r) = \frac{16\pi\gamma a R_1 R_2}{R_1 + R_2}\,\frac{1}{1+\exp[(r - R_1 - R_2 - \Delta R)/a]}.$$

Was developed to describe elastic scattering. It has the diffuseness $a \approx$ 0.65 fm, and an adjustable radius parameter ΔR. It is consistent with the M3Y double-folding potential near and outside the Coulomb barrier.

Standard two-phonon calculation of fusion.

Use iso-centrifugal approximation: one channel for each state.

Replace

$\lambda + 1$ channels

by 1 channel.

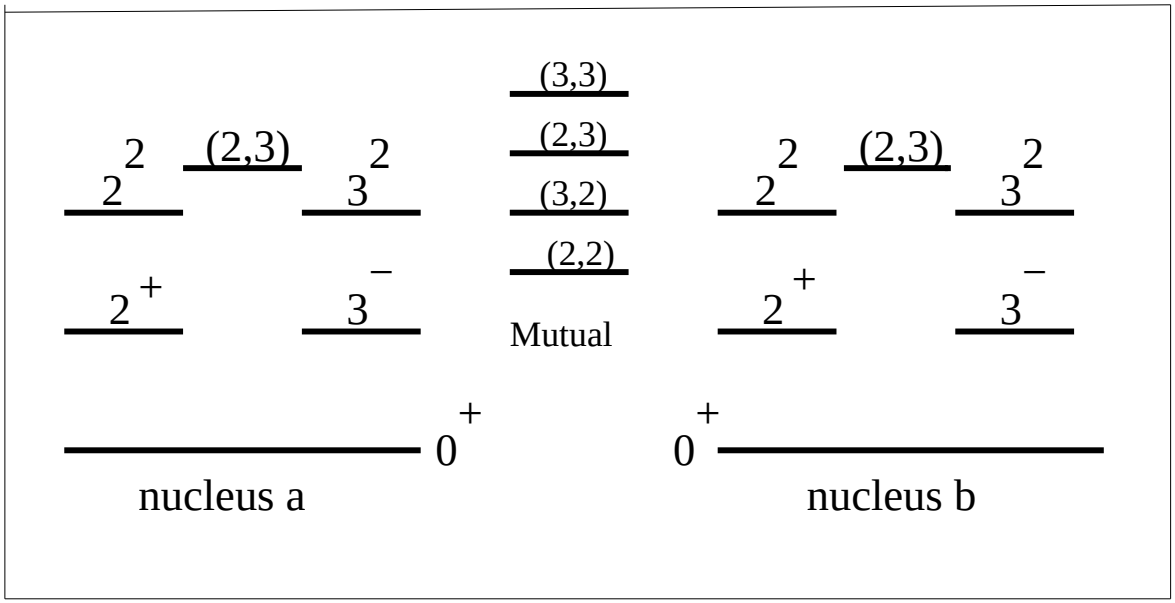

1 (GS) + 4 (1PH) + 4 (2PH) + 6 (Mutual) = 15 channels.

This model works quite well for the fusion of not too heavy systems.

- It does not work so well for heavy, soft or strongly deformed nuclei,
- in fusion reactions, where transfer with $Q_{tr} > 0$ plays a role.

Such a description usually explains the data at energies near and below the Coulomb barrier

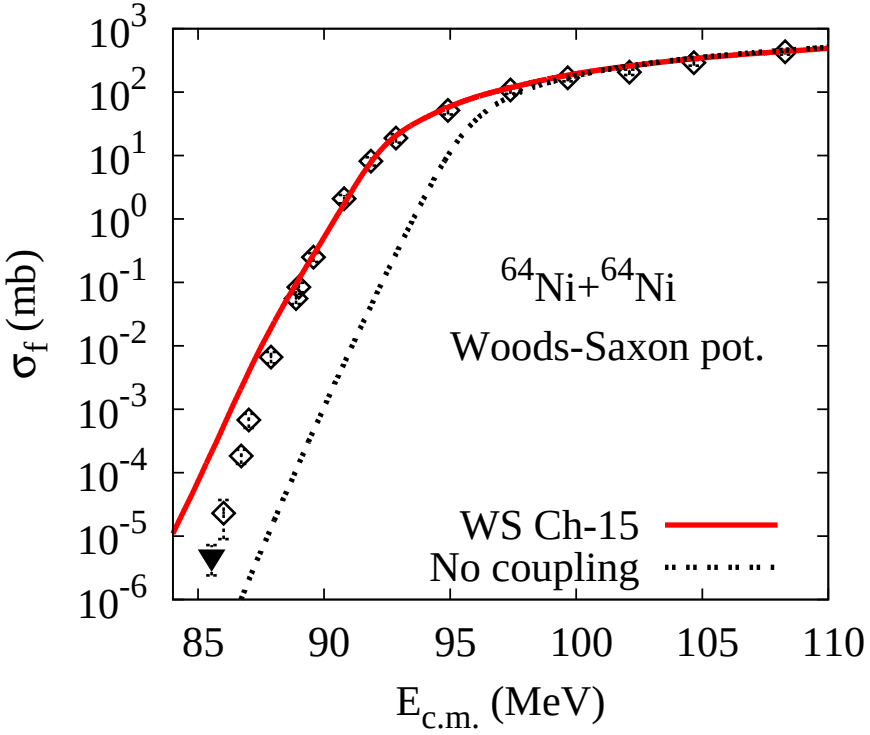

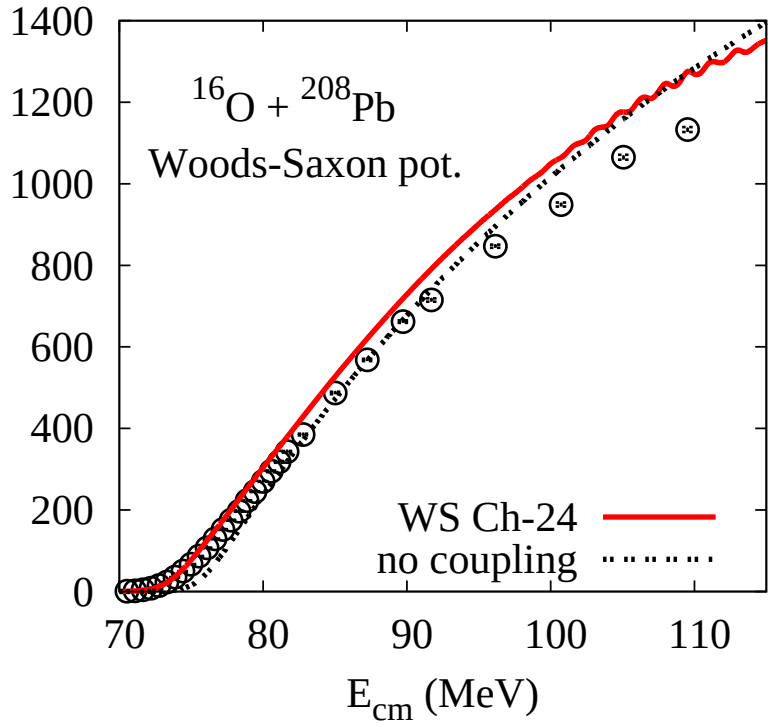

but not always **far below** or **far above** the Coulomb barrier.

^{64}Ni+^{64}Ni: V_{CB} = 95.2 MeV, ^{16}O+^{208}Pb: V_{CB} = 75.6 MeV.

^{64}Ni+^{64}Ni data by *Jiang et al.*, PRL 93, 012701 (2004).

^{16}O+^{208}Pb data by *Morton et al.*, PRC 60, 044608 (1999).

The M3Y double-folding potential.

$$U_N(\mathbf{r}) = \int d\mathbf{r}_1\, d\mathbf{r}_2\, \rho_a(\mathbf{r}_1)\, \rho_A(\mathbf{r}_2)\, v_{NN}(\mathbf{r} + \mathbf{r}_2 - \mathbf{r}_1).$$

The effective M3Y interaction produces a very realistic potential near and outside the barrier, and is consistent with the empirical Woods-Saxon potential. However, the entrance channel potential **is too deep.**

The M3Y+repulsion potential: Supplement the M3Y interaction with a repulsive term,

$$v_{NN}^{\rm rep} = v_{\rm rep}\, \delta(\mathbf{r} + \mathbf{r}_2 - \mathbf{r}_1).$$

Use a small, adjustable diffuseness of the densities, $a_r \approx 0.3$–0.4 fm, when calculating the repulsive part. Calibrate the strength $v_{\rm rep}$, so that the total nuclear interaction for overlapping nuclei is consistent with the Equation of State,

$$U_N(r = 0) = 2A_a[\epsilon(2\rho) - \epsilon(\rho)] \approx \frac{A_a}{9} K,$$

and nuclear incompressibility of $K \approx 234$ MeV (*Myers & Swiatecki*).

The M3Y+repulsion entrance channel potential.

Mişicu and Esbensen, PRL 96, 112701 (2006).

The shallow M3Y+repulsion potential has been adjusted to reproduce the fusion data.

Two adjustable parameters:
R and a_r.

The hindrance sets in below 89 MeV, far above the ground state of the compound nucleus.

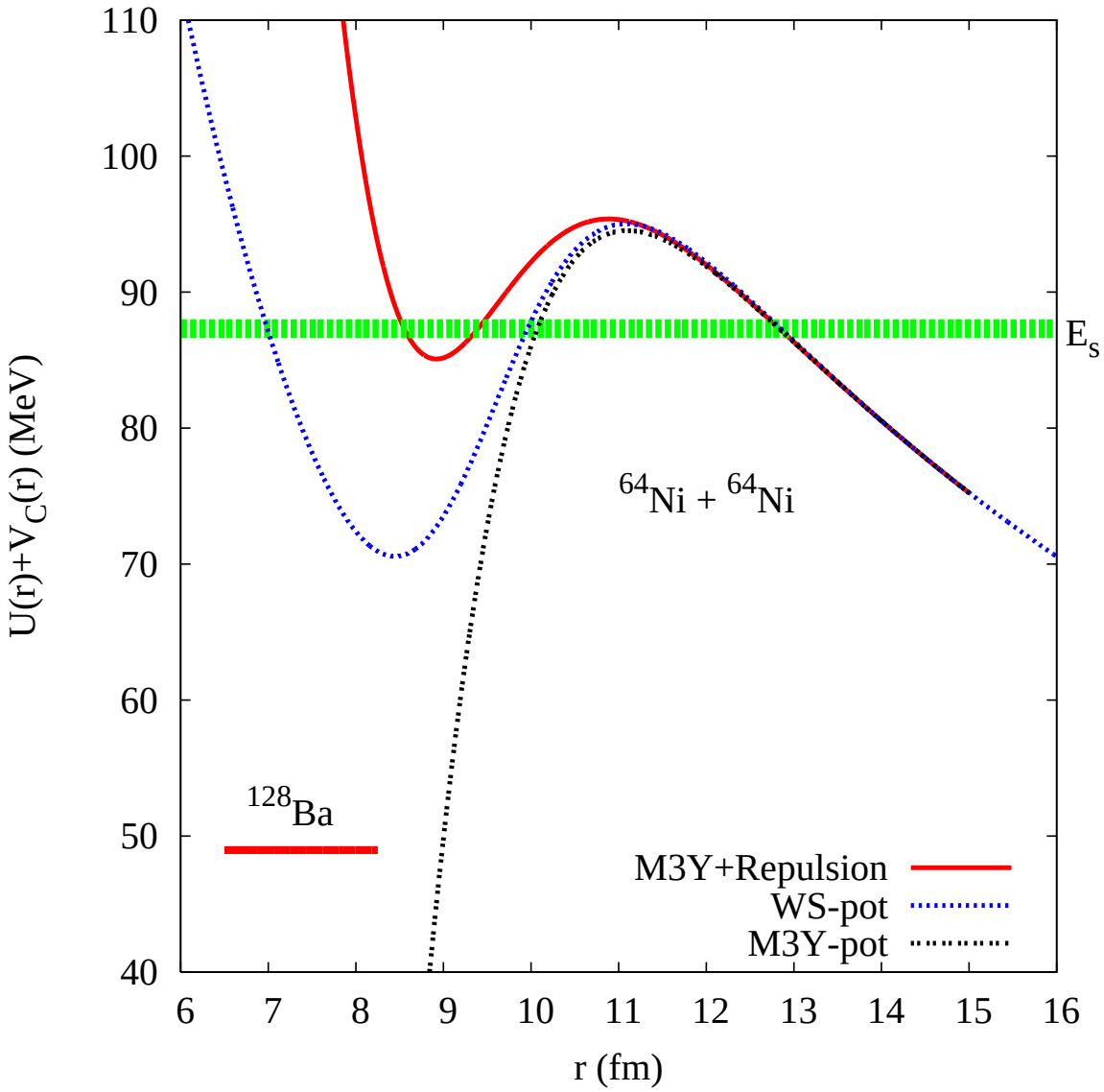

The data are explained by applying the M3Y+repulsion.

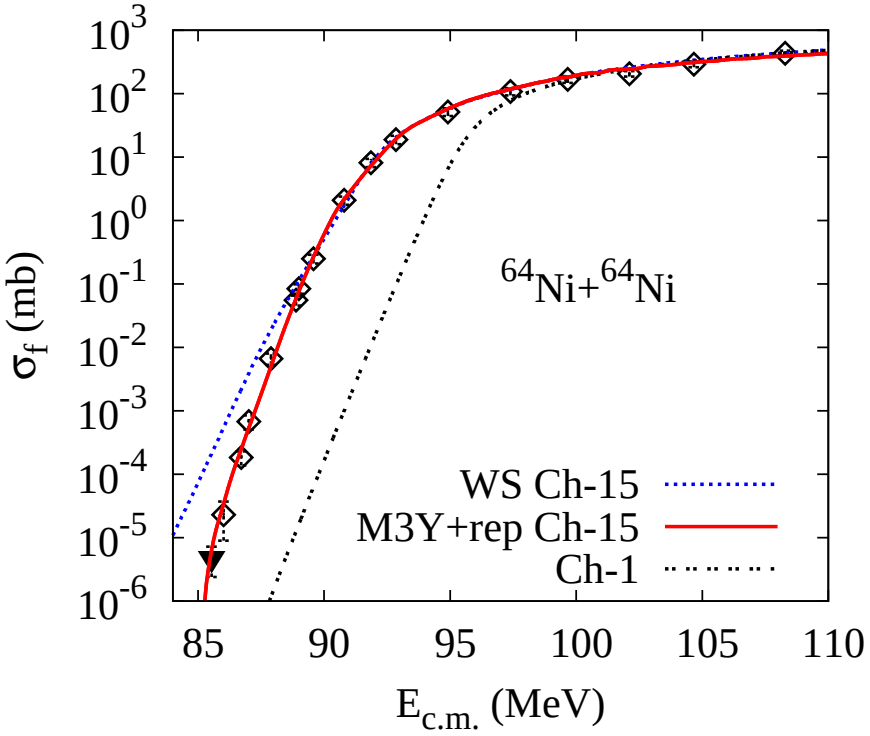

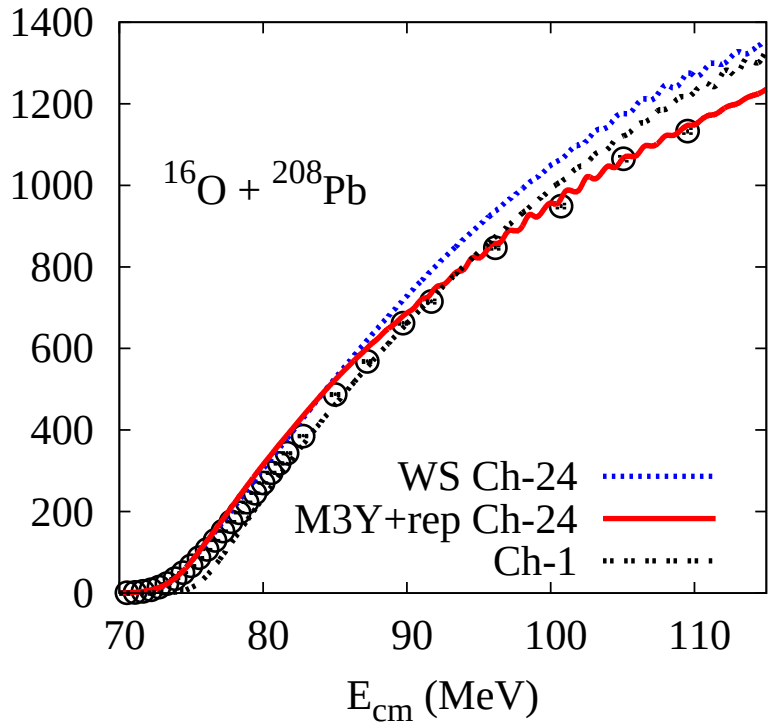

The M3Y+repulsion potential *"hits two flies with one swat."*

Explains the hindrance at very low energies

and the suppression at high energies.

Mişicu and Esbensen, PRL 96, 112701 (2006); PRC 76, 054609 (2007).

Advantages of using a double-folding potential

in coupled-channels analyses of heavy-ion fusion data.

- If the densities of the reacting nuclei are known, one can predict the ion-ion potential. *One can then focus on the structure input.*
- Extract the densities of the reacting nuclei from the analysis of the fusion data. *If the extracted density is poor, the nuclear structure input could be poor or incomplete.*
- Applications to the fusion of calcium isotopes: extract the densities of ^{40}Ca and ^{48}Ca from the ^{40}Ca+^{40}Ca and ^{48}Ca+^{48}Ca fusion data. *Predict the ion-ion potential for ^{40}Ca+^{48}Ca and compare the calculated fusion cross section to data.* **Does it work?**

Analysis of ^{48}Ca+^{48}Ca fusion data.

Experiment: *Stefanini et al.*, PLB 679, 95 (2009).

Calculations: *Esbensen et al.*, PRC 82, 054621 (2010).

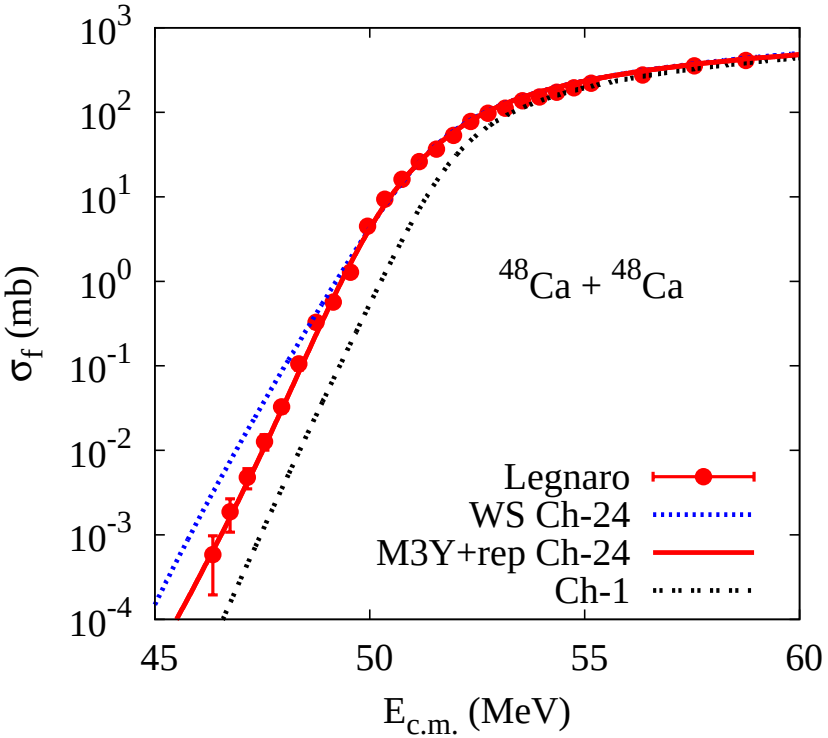

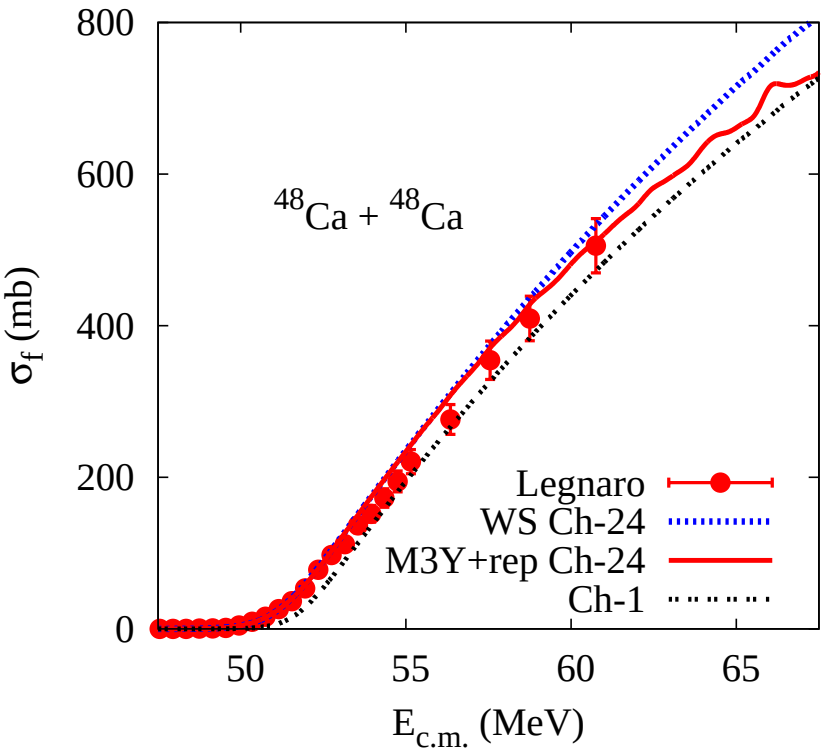

The data are hindered at low energy and suppressed at high energy with respect to the Woods-Saxon based calculation.

The shallow M3Y+repulsion potential provides much better agreement.

Analysis of ^{40}Ca+^{40}Ca fusion data.

Legnaro data: *Montagnoli et al.*, PRC 85, 024607 (2012);

older MIT data: *Aljuwair et al.*, PRC 30, 1223 (1984).

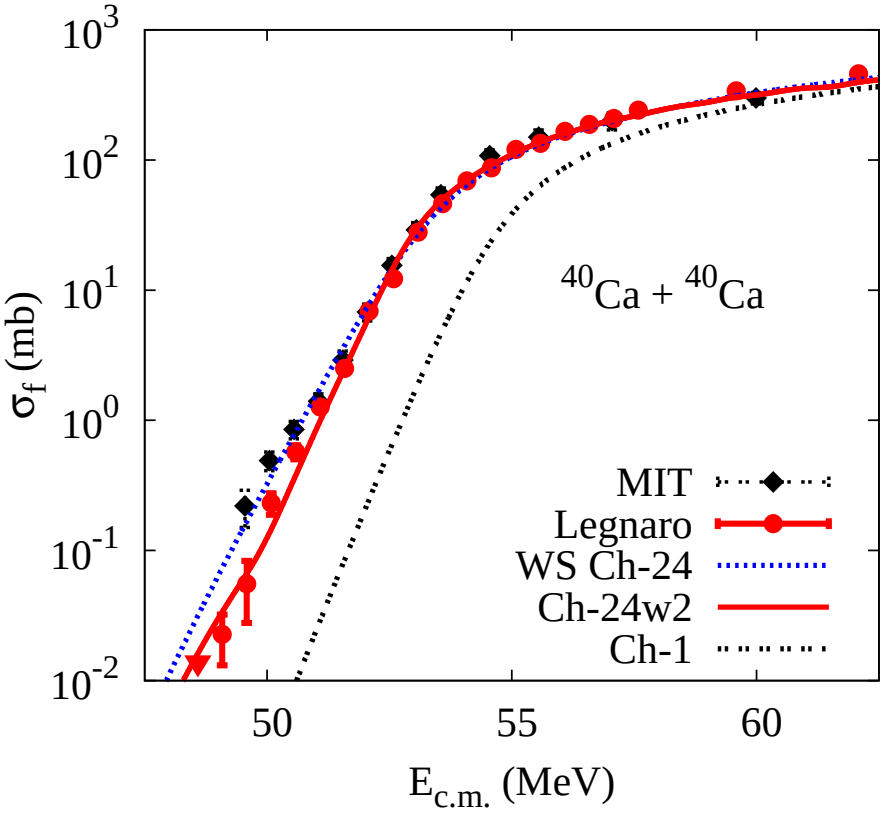

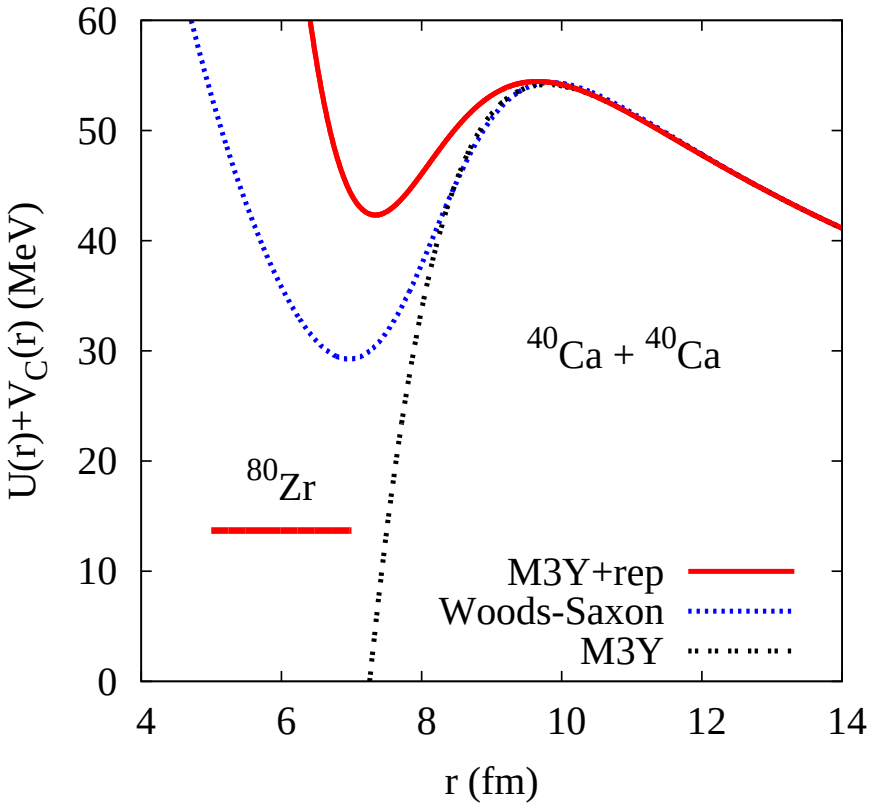

The Legnaro data are hindered with respect to the WS based calc.

The M3Y+rep potential gives a better account of the Legnaro data.

Extracted densities of the calcium isotopes.

Are they realistic?

Compare the RMS radii to the point-proton and point-nucleon RMS radii, obtained from electron and proton scattering experiments, or to the predictions Hartree-Fock (HF) calculations.

Nucleus	Fusion	point-proton	point-nucleon	HF (Negele)
^{40}Ca	3.40	3.383(1)	3.44(5)	3.39
^{48}Ca	3.56	3.387(1)	3.53(3)	3.58

If the extracted radius is too large: couplings too weak.
If the extracted radius is too small: couplings too strong.

The RMS radii extracted from the fusion data are reasonable, so the nuclear structure input must have been reasonable.

Analysis of ^{40}Ca+^{48}Ca fusion data.

Legnaro data: *Jiang et al.*, PRC 82, 041601 (2010),

MIT data: *Aljuwair et al.*, PRC 30, 1223 (1984).

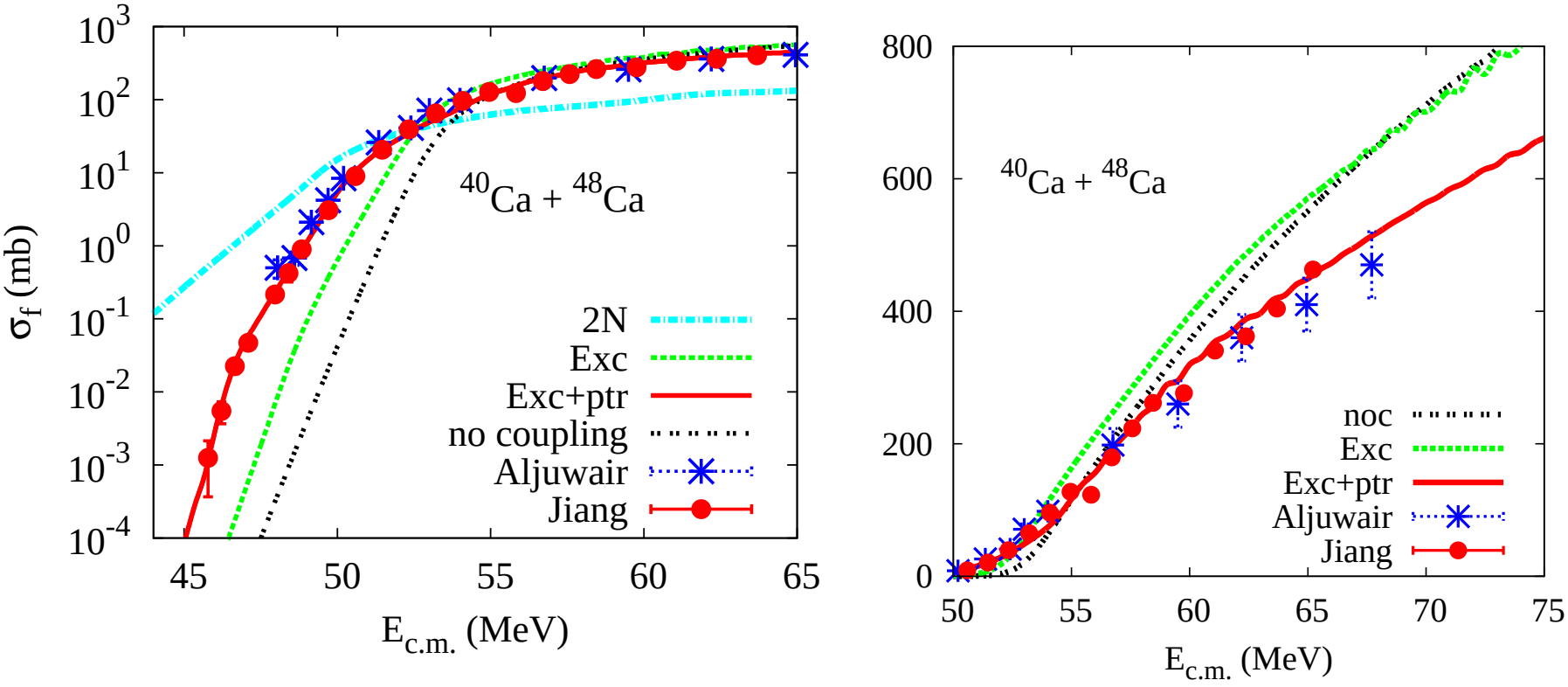

The prediction based on excitations alone

is too low at low energies and too high at high energies.

Couplings to $1N$ and $2N$ transfer are needed to explain the data.

Influence of transfer on the fusion of ^{40}Ca+^{48}Ca:

Q-values for pair transfer are positive: Q_{2n} = 2.6 MeV, Q_{2p} = 7.1 MeV.
That can cause a large enhancement of subbarrier fusion.
The influence of $2N$ pair-transfer is simulated by the form factor,

$$F_{2N}(r) = -\sigma_{tr}\frac{dU(r)}{dr}.$$

Adjust the strength (σ_{tr}=0.39 fm) so that the fusion data are reproduced.
Excitations and transfer are treated as independent degrees of freedom.

Ground state Q-values for transfer are large and negative for
^{40}Ca+^{40}Ca ($Q_{tr} \leq$ -7 MeV) and ^{48}Ca+^{48}Ca ($Q_{tr} \leq$ -5 MeV).
The influence of transfer on fusion must be weak.
Consistent with the analysis which did not include/need any transfer.

Isotope dependence of Ca+Ca fusion cross sections.

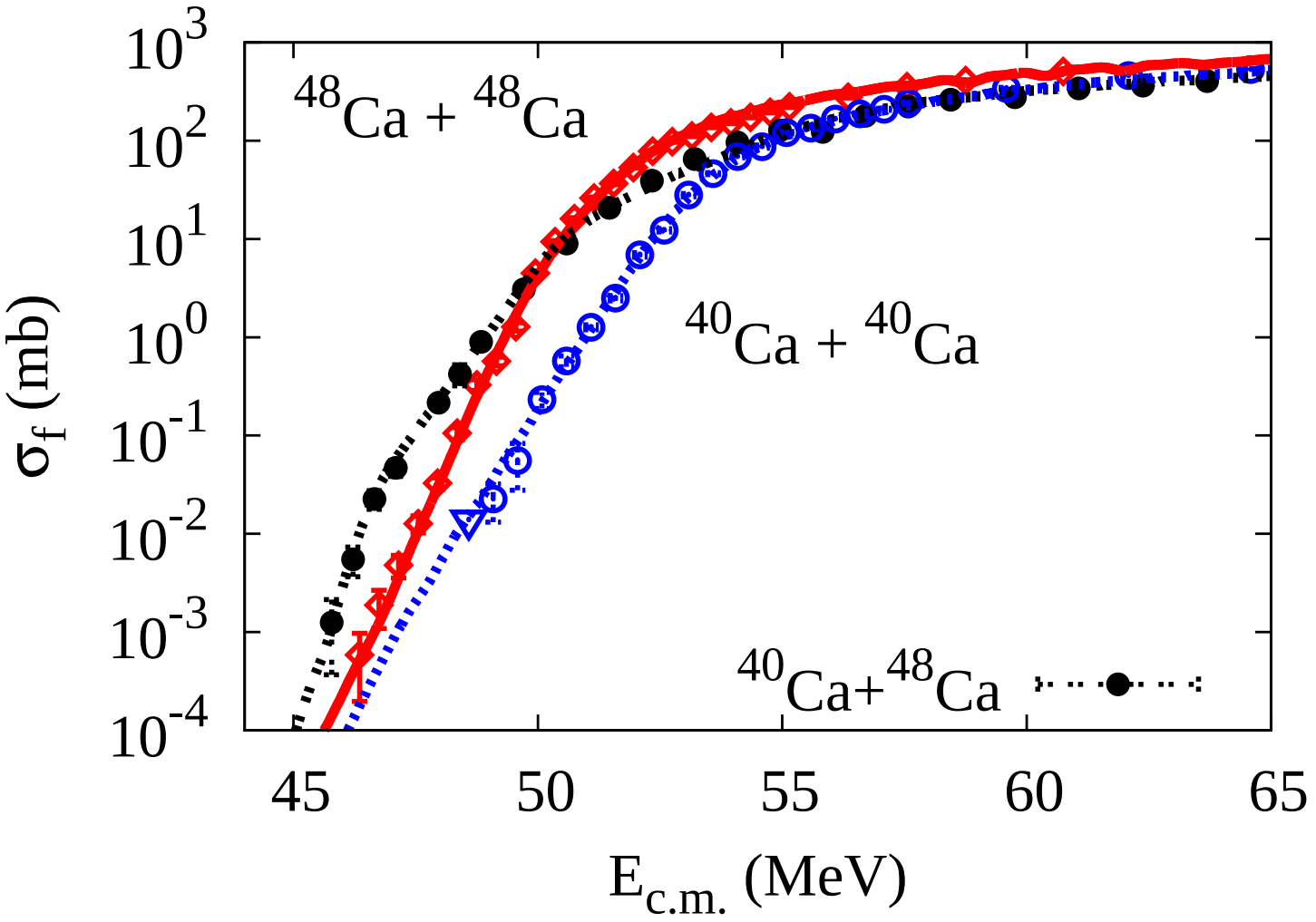

The ^{40}Ca+^{48}Ca cross sections exceed the ^{48}Ca+^{48}Ca data at low energy, but are suppressed compared to the ^{40}Ca+^{40}Ca data at high energy.

Fusion Reactions with Carbon Isotopes

Esbensen, Tang, & Jiang, PRC 84, 064613 (2011).

Problems:

Large structures in $^{12}C+^{12}C$ fusion data.

Large systematic uncertainties of 15% or more. Modified data: *

Analyze instead a **smooth** cross section, e. g., for the fusion of $^{13}C+^{13}C$, and **predict** the cross section for the fusion of $^{12}C+^{12}C$.

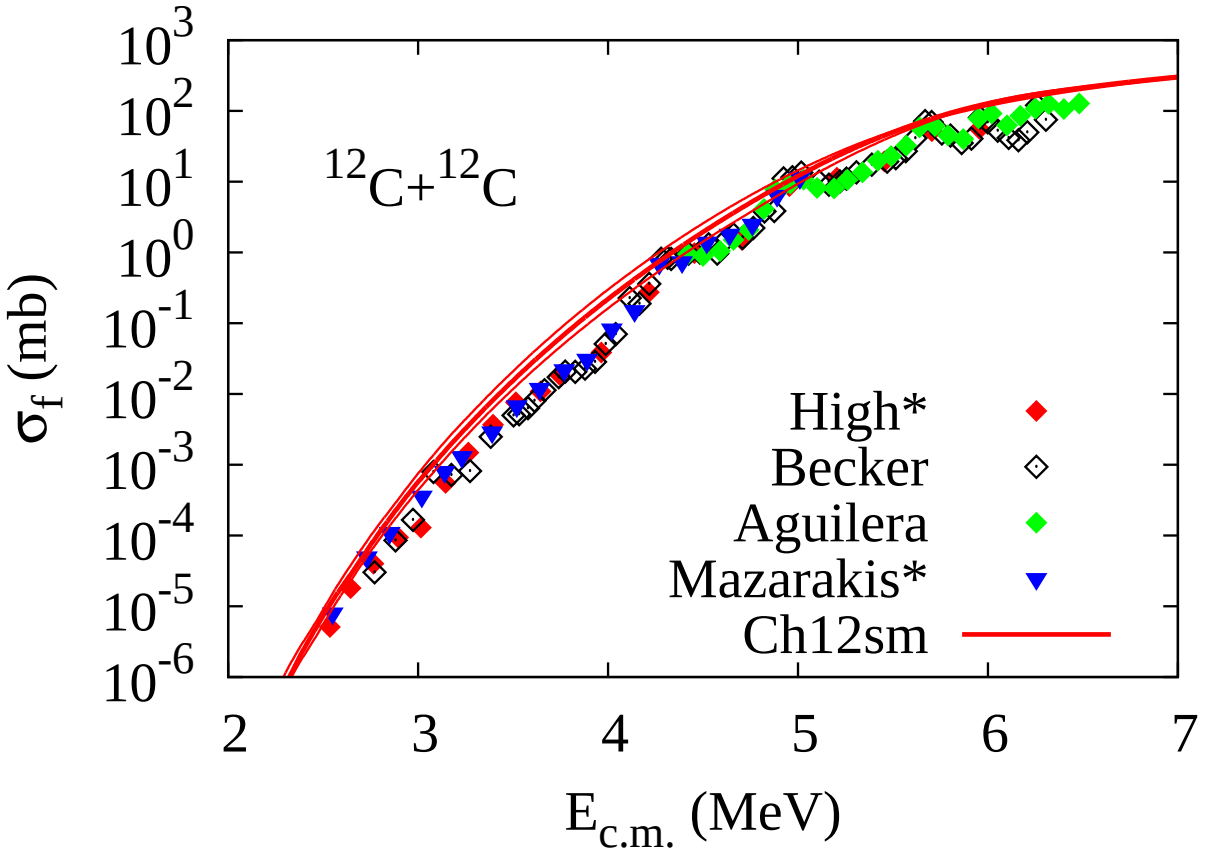

Fusion of ^{13}C+^{13}C.

Best fit to Trentalange's ^{13}C+^{13}C fusion data.

Trentalange et al., NPA 483, 406 (1988).

Excellent fit to the shape of the data is achieved by adjusting the ion-ion potential. Best fit to Trentalange's data for S_c = 0.85.

Best fit to Charvet's data for S_c = 0.96.

Charvet et al., NPA 376, 292 (1982).

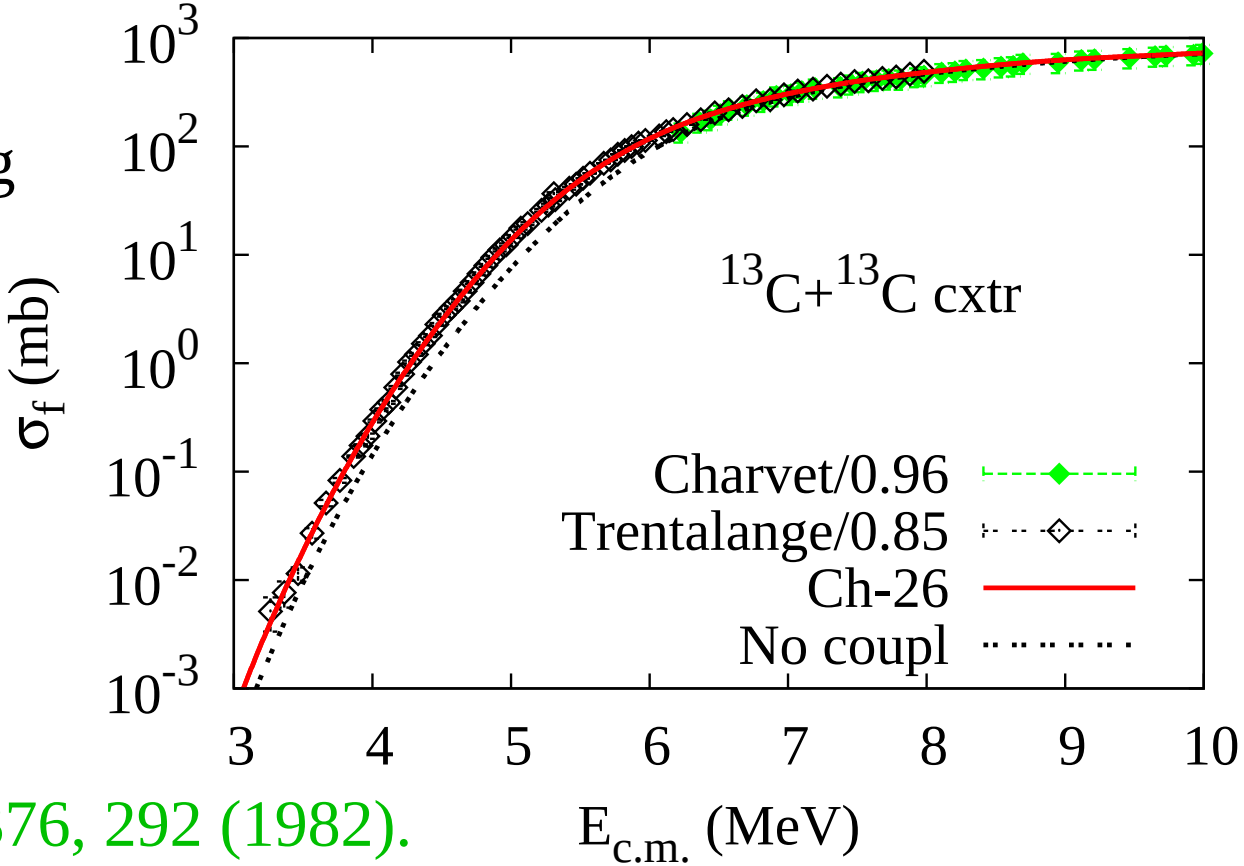

Coupling Scheme for ^{13}C+^{13}C reactions.

Ch-13 calculations: include all states below 10 MeV.

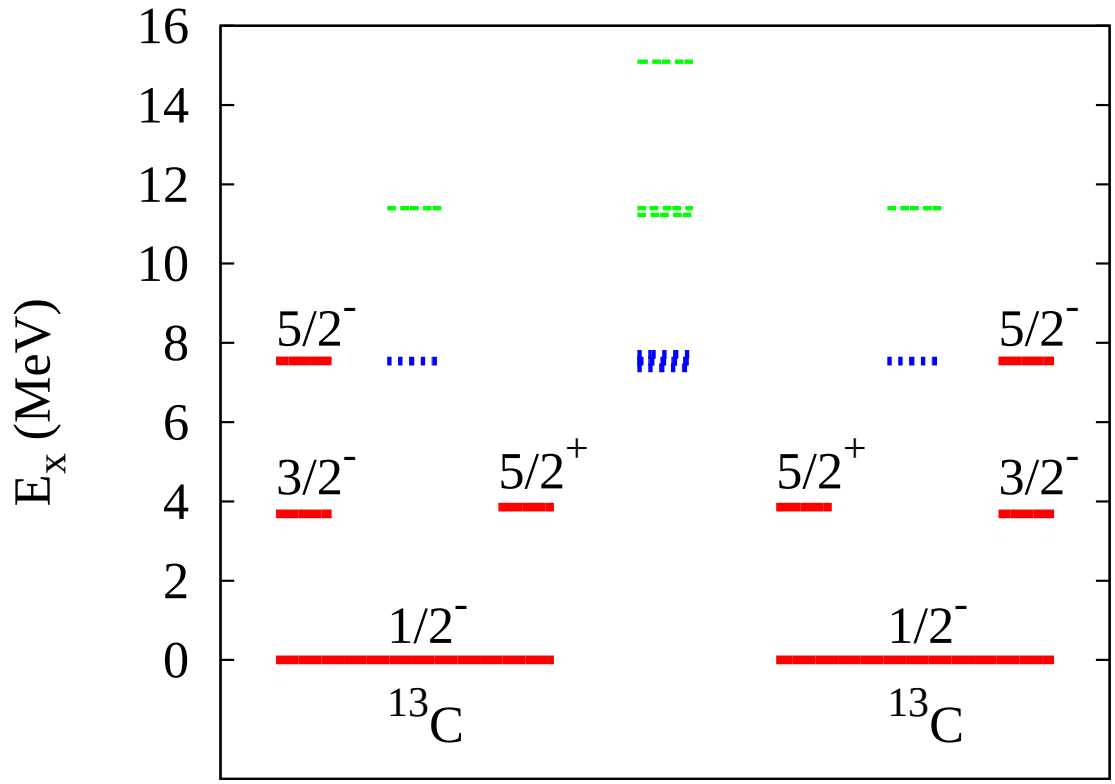

Ch-26 calculations: include in addition one-neutron transfer.

Q_{1n}=3.2 MeV. *Assume independent modes of excitation and transfer.*

Entrance Channel Potential for ^{13}C+^{13}C fusion.

M3Y+repulsion, double-folding potential.

Density parameters: R = 2.285 fm, a = 0.44 fm, a_r = 0.31 fm.

V_{CB} = 6.05 MeV.

V_{min} = -12.00 MeV.

Coupled-channels calc.:
use **ingoing-wave boundary conditions** at the pocket minimum.
Fusion is determined by the **ingoing flux.**

Closed channels:
treated as decaying states when $E_{c.m.} \leq E_x$ (Whittaker function.)

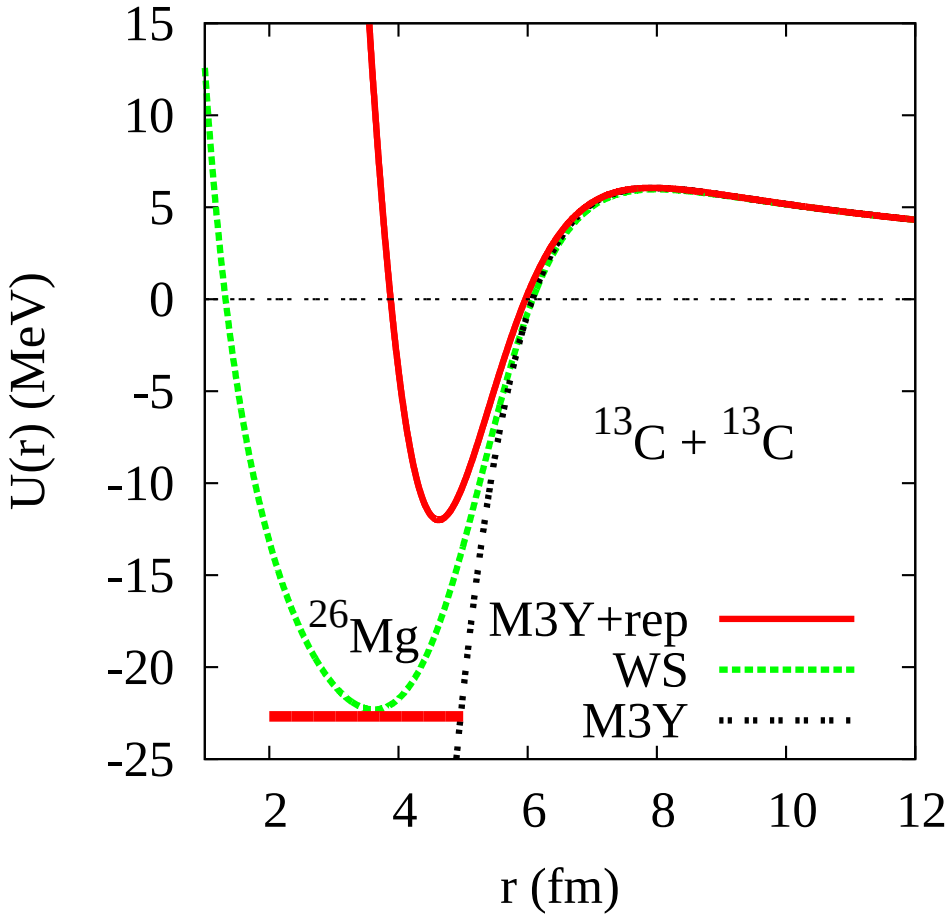

Large sensitivity to two-phonon excitations.

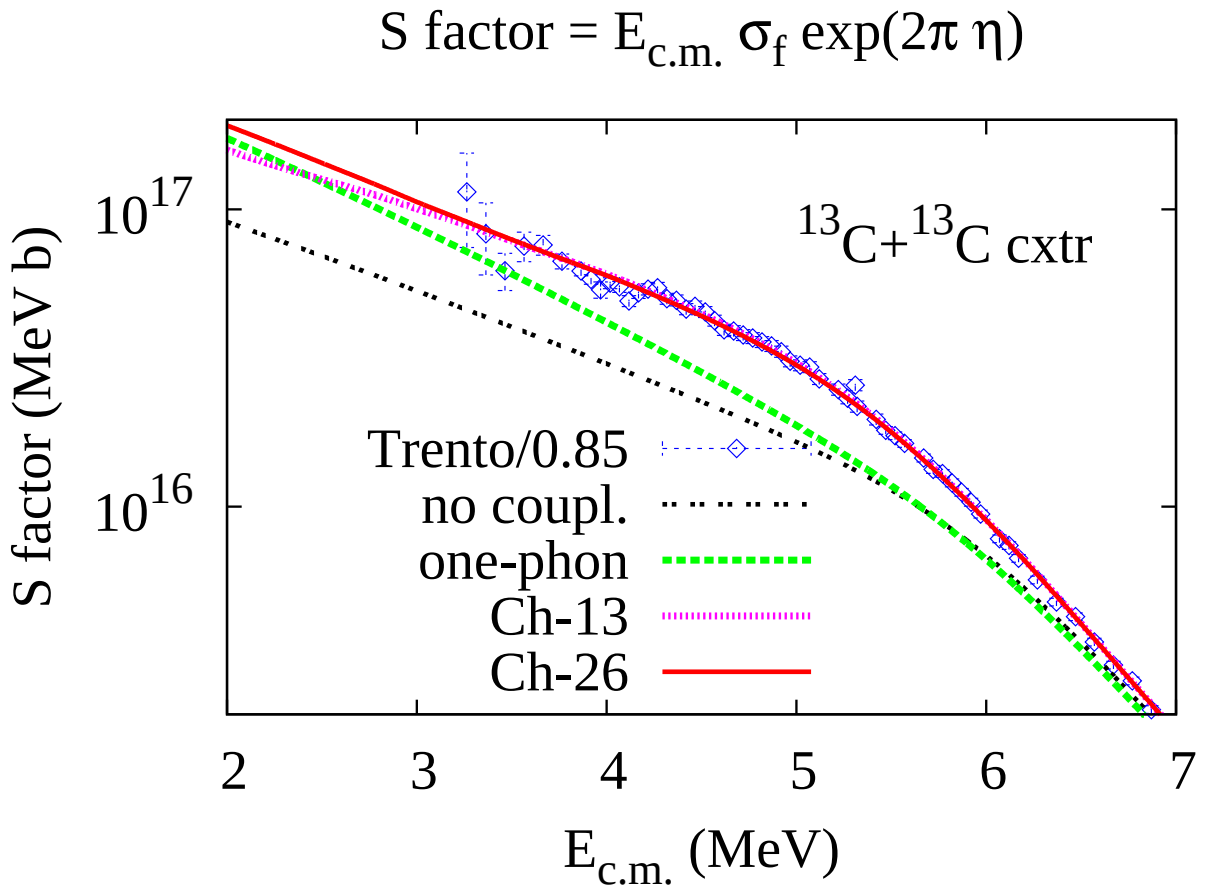

The one-phonon calculation rises too slowly.

Ch-13: The two-phonon calculation gives an excellent fit.

Ch26: Small effect of transfer. Minor structures in the data.

Prediction of $^{12}C+^{13}C$ fusion.

Comparison to Dayras's data,

Dayras et al., NPA 265, 153 (1976).

Best fit to Dayras's data is achieved for S_c = 1.01.

Best fit to Notani's data is achieved for S_c = 1.17.

Notani et al., PRC 85, 014607 (2012).

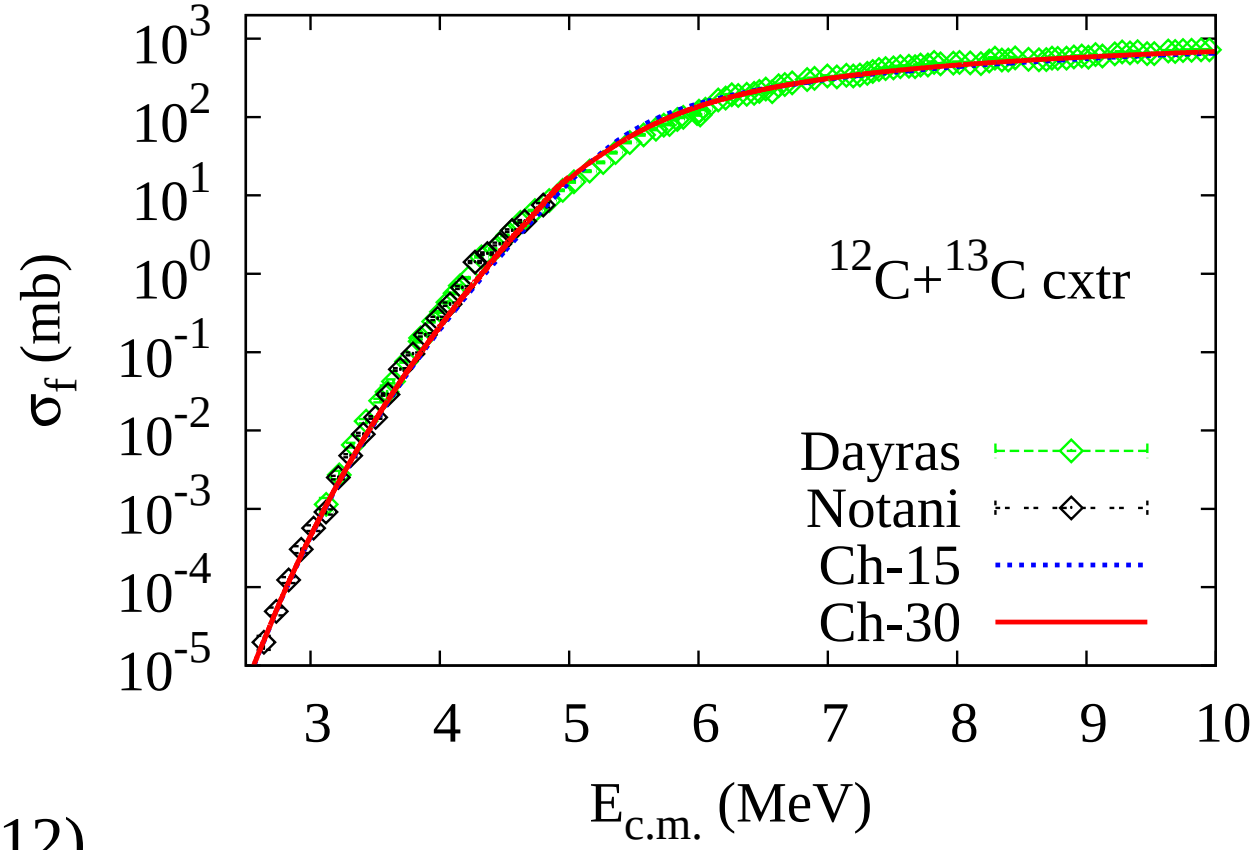

However, they were normalized to Dayras's low-energy data.

Irregular normalization of fusion data.

Esbensen, Tang, & Jiang: PRC 84, 064613 (2011).

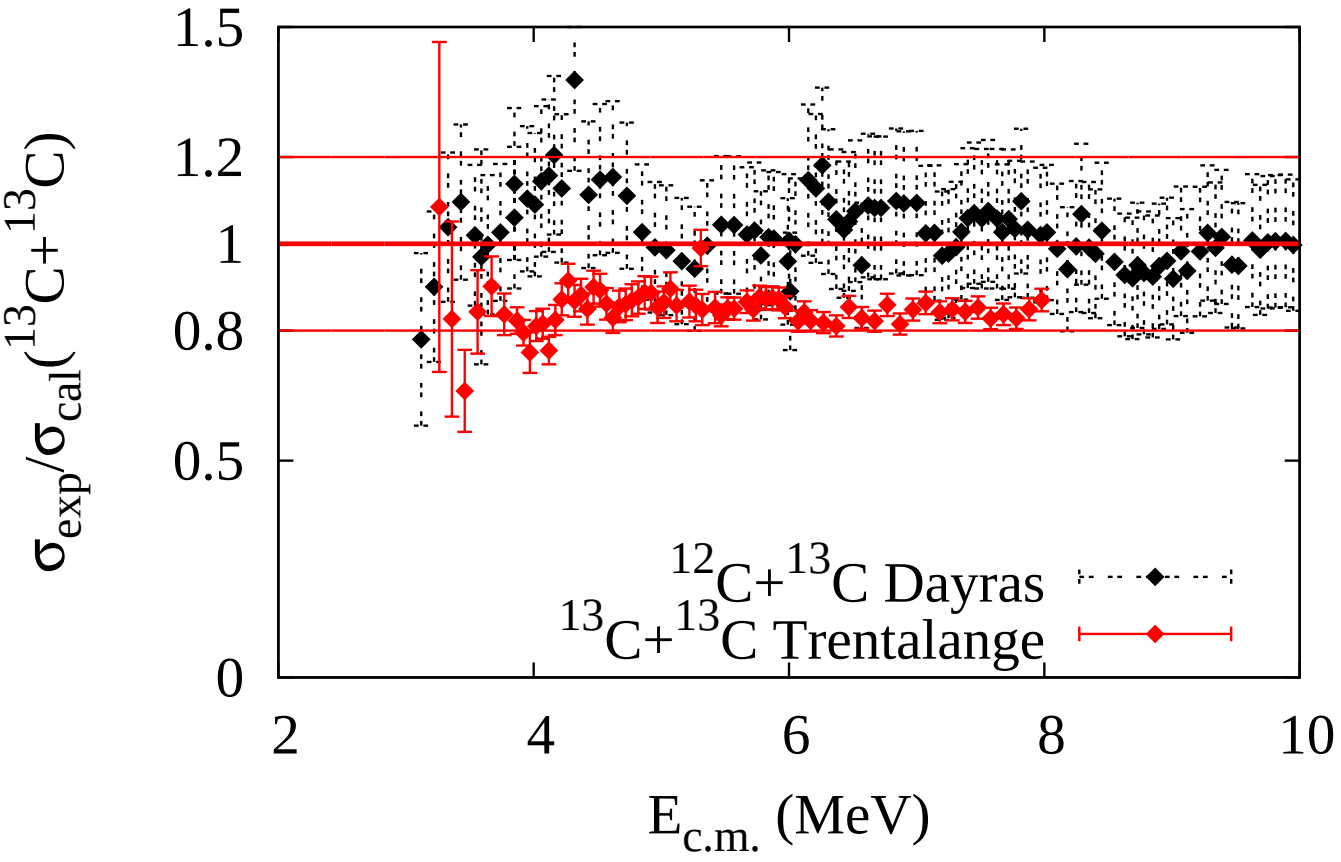

The two data sets are normalized to the same $^{13}C+^{13}C$ calculation.

Why are the data lower for the larger systems?

Nuclear Structure Input for ^{12}C

to coupled-channels calculations.

Properties of E2 and E3 transitions to the low-lying states.

State	E_x (MeV)	Transition	B(Eλ) (W.u.)	β_λ
2^+	4.439	E2: $0_1^+ \rightarrow 2^+$	4.65(26)	0.570
0_2^+	7.654	E2: $2^+ \rightarrow 0_2^+$	8.0(11)	0.236
3^-	9.641	E3: $0_1^+ \rightarrow 3^-$	12(2)	0.90(7)

Note that β_3 = 0.90(7) is extremely large,

and $E_x(3^-)$ = 9.64 MeV is quite high.

Note that all inelastic channels are closed for $E_{cm} < 4.4$ MeV.

Use decaying state boundary conditions for closed channels.

Coupling Scheme for ^{12}C+^{12}C calculations

Assume independent modes of excitation.

$\beta_2 = 0.57$

$\beta_3 = 0.90(7)$

Ch-10: all red states.

Ch-12SM:

Add the mutual $(2^+, 3^-)$ excitation in each nucleus but only with half strength. Suggested by shell model calculations of the $(2^+, 3^-)_{4^-}$ state state in ^{12}C (Alex Brown).

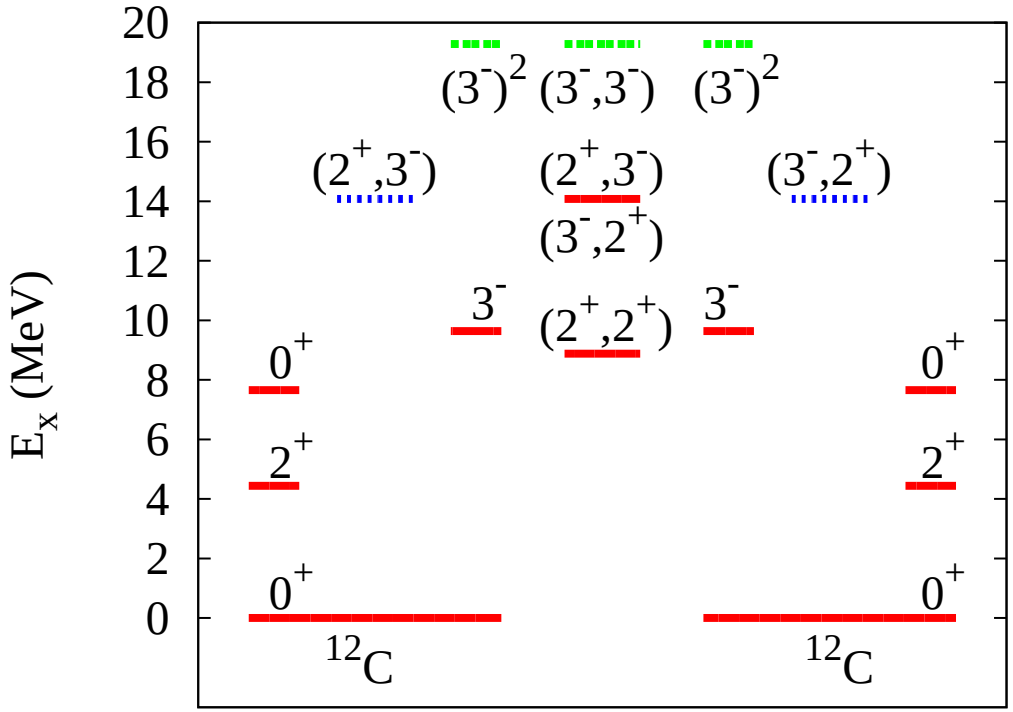

Ignore the two-phonon $(3^-)^2$ and mutual $(3^-,3^-)$ excitations.

The excitation energy is very high.

Prediction of ^{12}C+^{12}C fusion

using the point-proton density and a_r = 0.31 fm.

Error band from

$\beta_3 = 0.90 \pm 0.06$

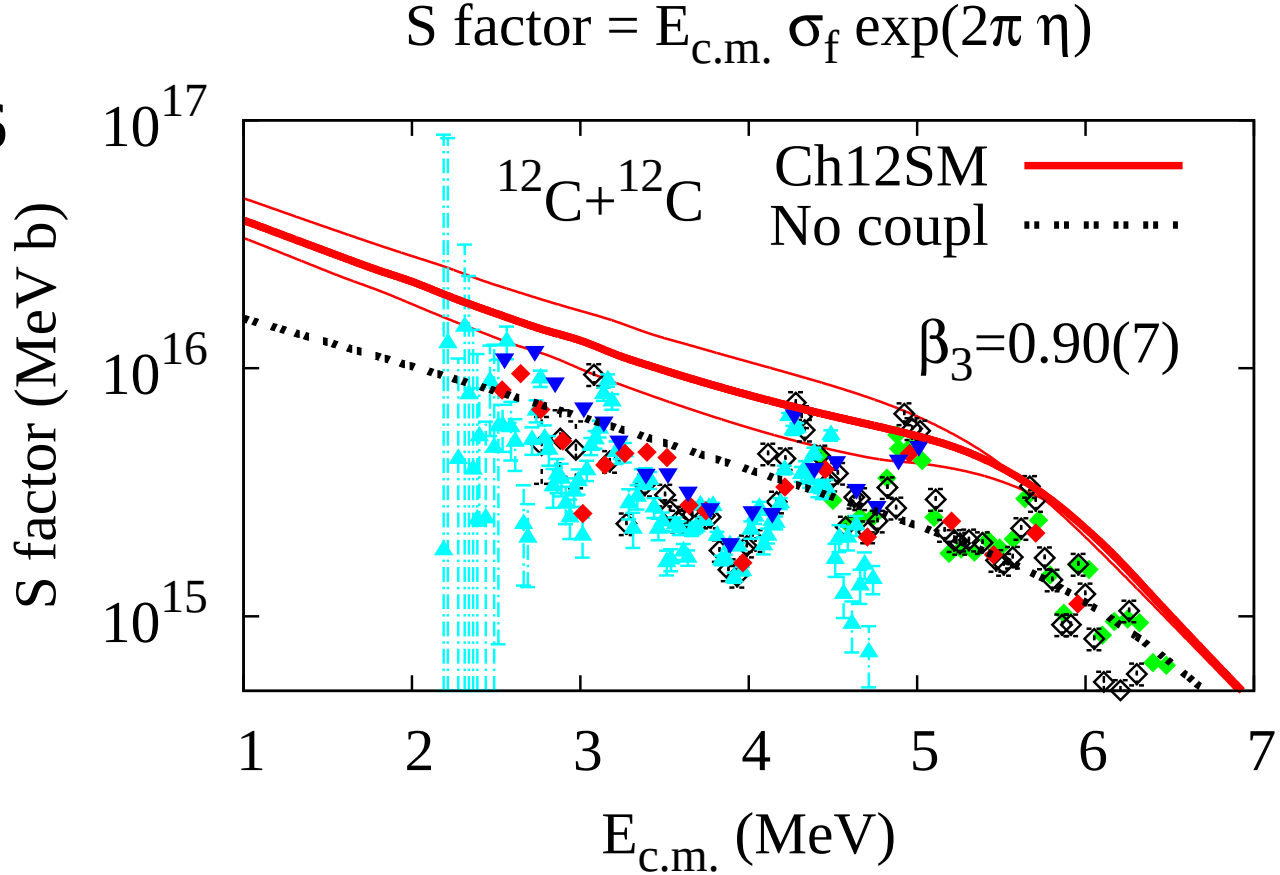

The Ch-12SM calculations is consistent with the maxima of the peaks.

Note: the no-coupling limit is not the background.

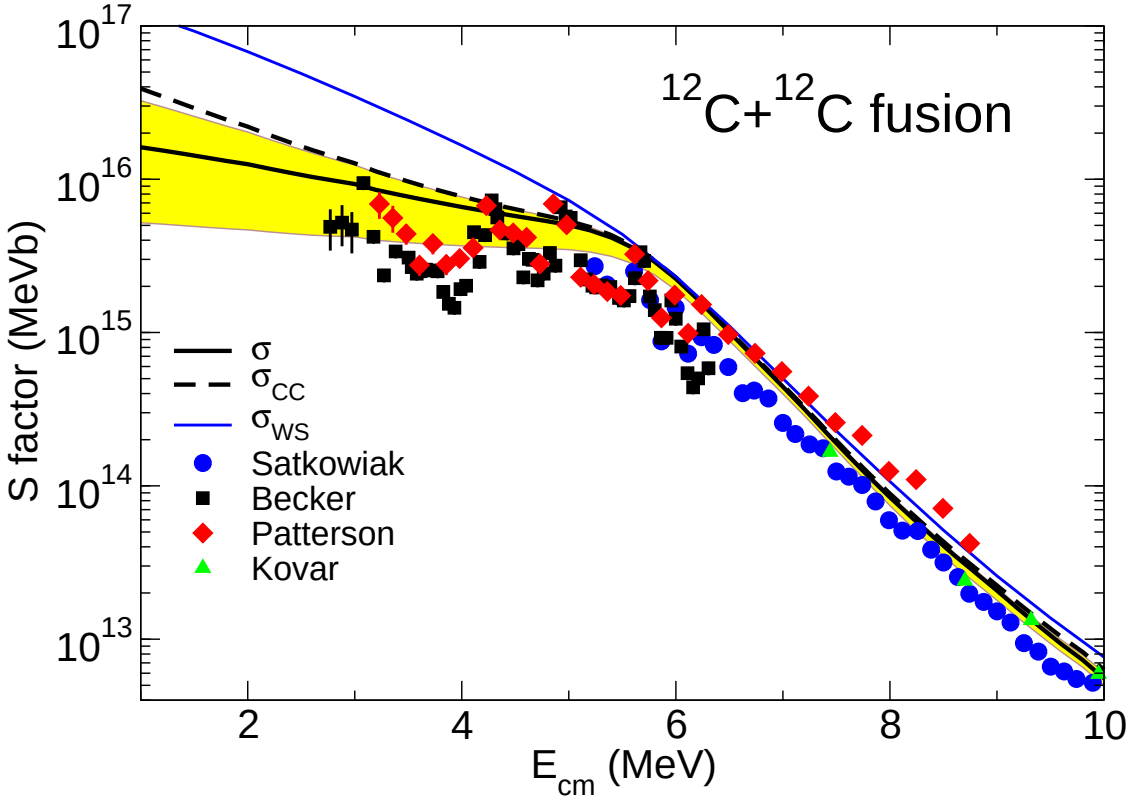

The 'suppression' of the data compared to the calculation σ_{CC} is caused by the low level density of 0^+, 2^+ and 4^+ states in ^{24}Mg,

$$\sigma_{fus}(E) = \frac{\pi}{k^2} \sum_J (2J+1)\, P_{fus}(E,J)\, P_{CN}(E,J).$$

Moldauer (1967): $P_{CN} = 1 - \exp(-2\pi\Gamma_J/D_J)$.

Jiang et al., PRL 110, 072701 (2013).

Systematics of Carbon Fusion.

Error band:

$\beta_3 = 0.90 \pm 0.07$

in ^{12}C.

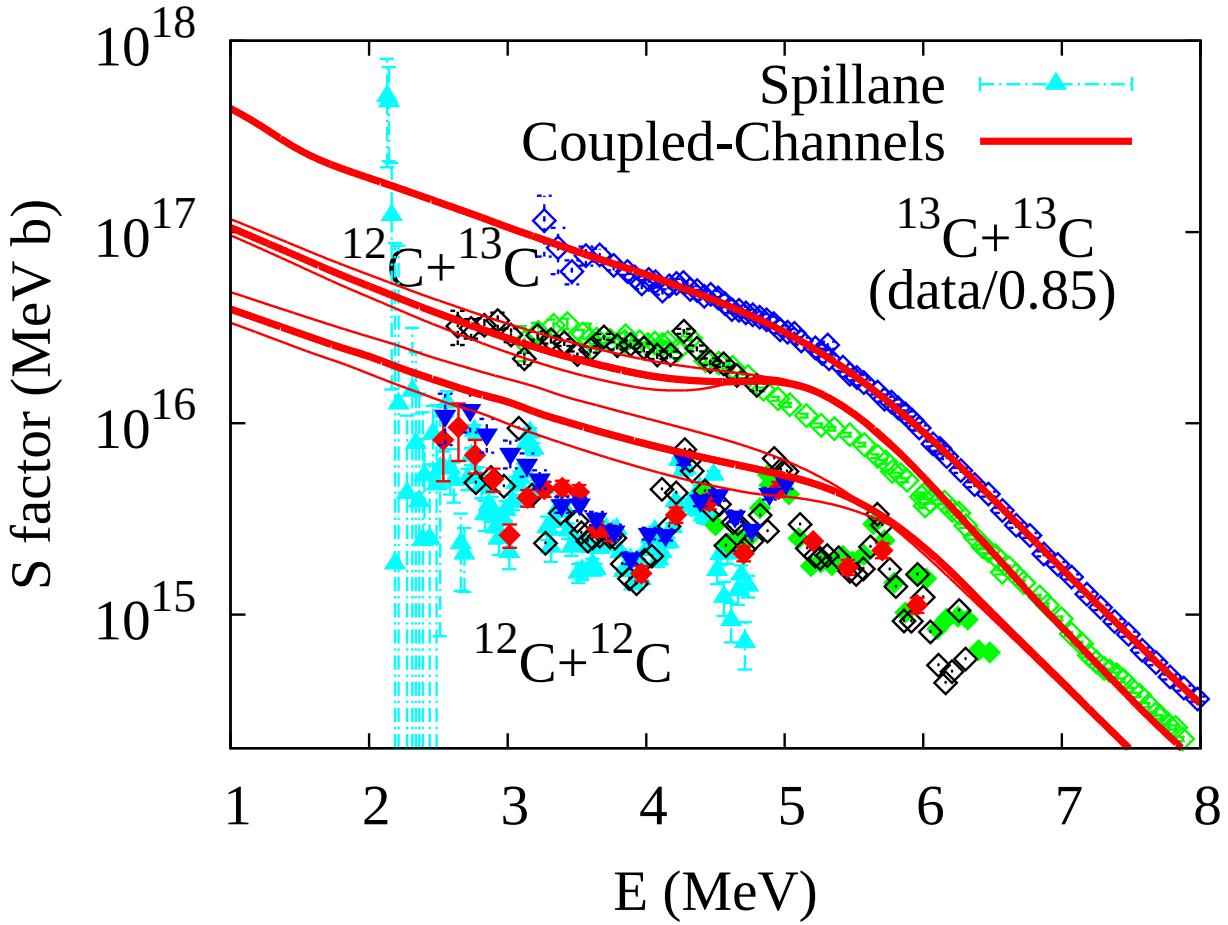

Coupled-channels calculations based on Ingoing-wave boundary conditions provide a consistent description of the carbon fusion data.

They provide an **upper limit** for the ^{12}C+^{12}C fusion data.

Spillane's lowest two points are 'too high'.

Conclusions.

- The **hindrance of fusion data** far below the Coulomb barrier and the **suppression** at high energy are general phenomena when compared to calculations that are based on a standard Woods-Saxon potential.
- They can both be explained by coupled-channels calculations that are based on the shallow **M3Y+repulsion** potential.
- Fusion is simulated by **IWBCs** that are imposed at the minimum of the pocket in the entrance channel potential, supplement with short-ranged **imaginary potential** at high energies.
- Include one-, two- and sometimes three-phonon excitations plus **transfer channels** with positive Q-values. That provides a consistent description of the Ca+Ca and Ca+Zr fusion data, with the exception of the ^{40}Ca + ^{96}Zr data, where the influence of transfer is expected to be very strong...

- **A consistent description** of the carbon fusion data is achieved.
  Use *Shell Model prediction* of the mutual $(2^+, 3^-)$ excitation in ^{12}C.
- **Structures in the low-energy ^{12}C+^{12}C fusion data** are not resonances. They are canyons that **are caused by** the hindrance due to **the low level density** of 0^+, 2^+, and 4^+ states in ^{24}Mg.
- The assumptions:
  1) the system is trapped after barrier penetration,
  2) the structure of the reacting nuclei does not change,
  3) excitations and transfer are independent modes,
  provide a fairly good description of most fusion data.
- There is apparently no need to follow the fusion dynamics all the way to the compound nucleus.

Argonne NATIONAL LABORATORY

Evidence of a shallow potential in high energy fusion.

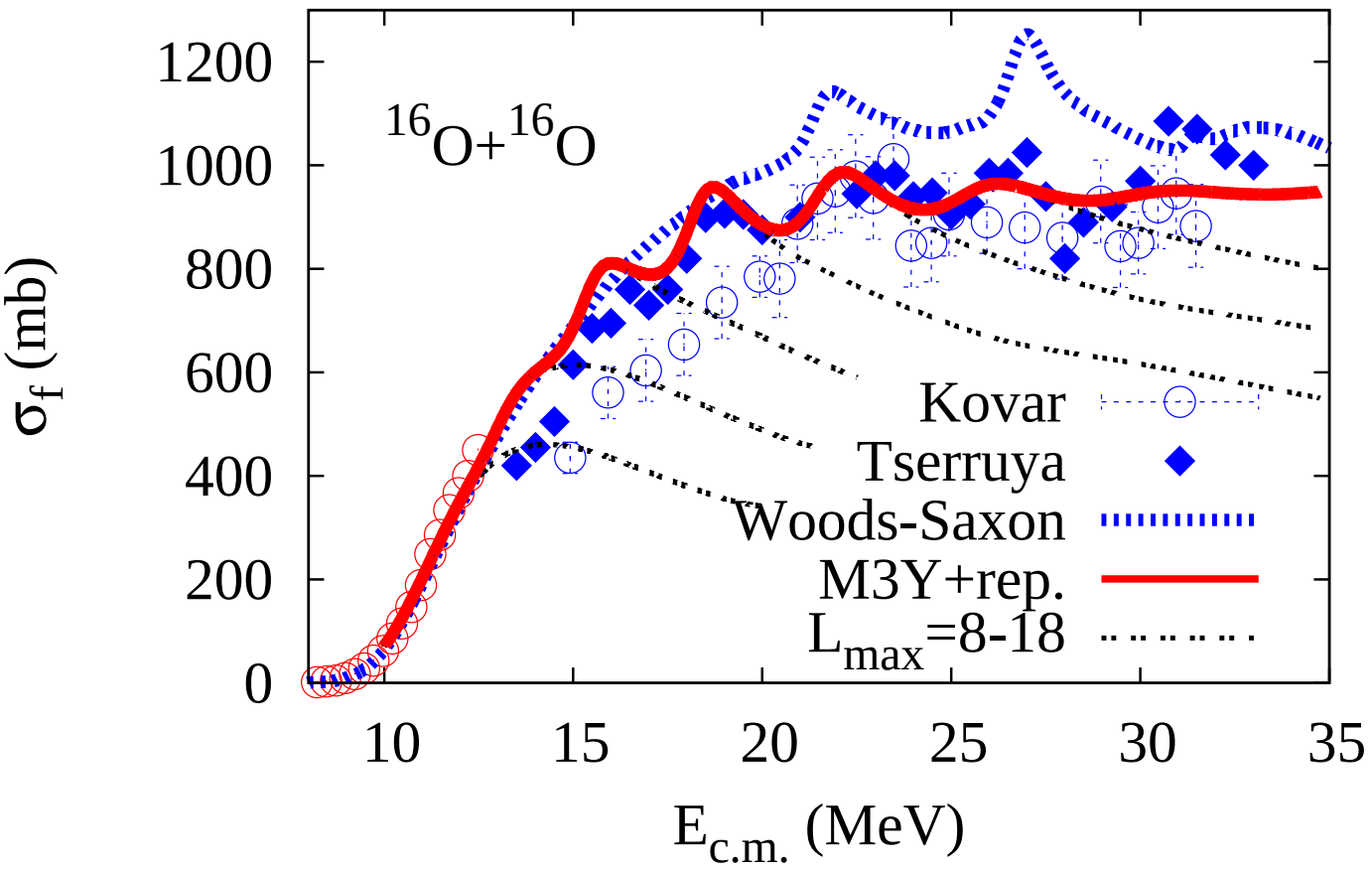

Coupled-channels calculations that are based on the shallow M3Y+repulsion potential provide a good description of the data by

Tserruya et al., PRC 18, 1688 (1978).

Calculations by *Esbensen*: PRC 77, 054608 (2008).

Effective centrifugal barriers are revealed in a $d(E\sigma_f)/dE$ plot.
Calculations by *Esbensen*: PRC 85, 064611 (2012).

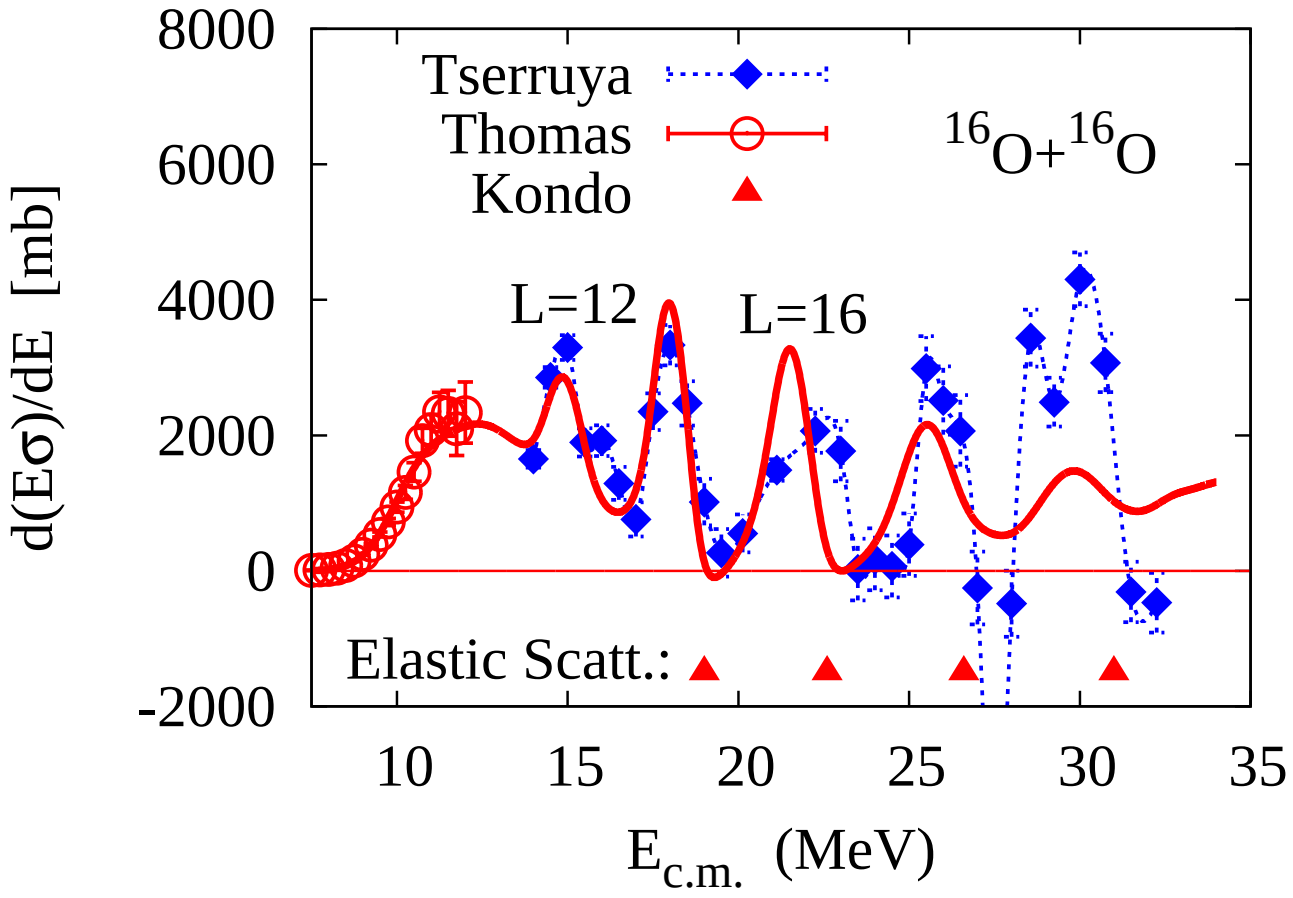

Well separated centrifugal barriers are observed for L = 12 - 20.
The peaks are consistent with the elastic scattering resonances found by *Kondo*, *Bromley*, *& Abe*, PRC 22, 1068 (1980).

High energy fusion of $^{12}C+^{12}C$.

Kovar et al., PRC 20, 1305 (1979.) The data are suppressed.

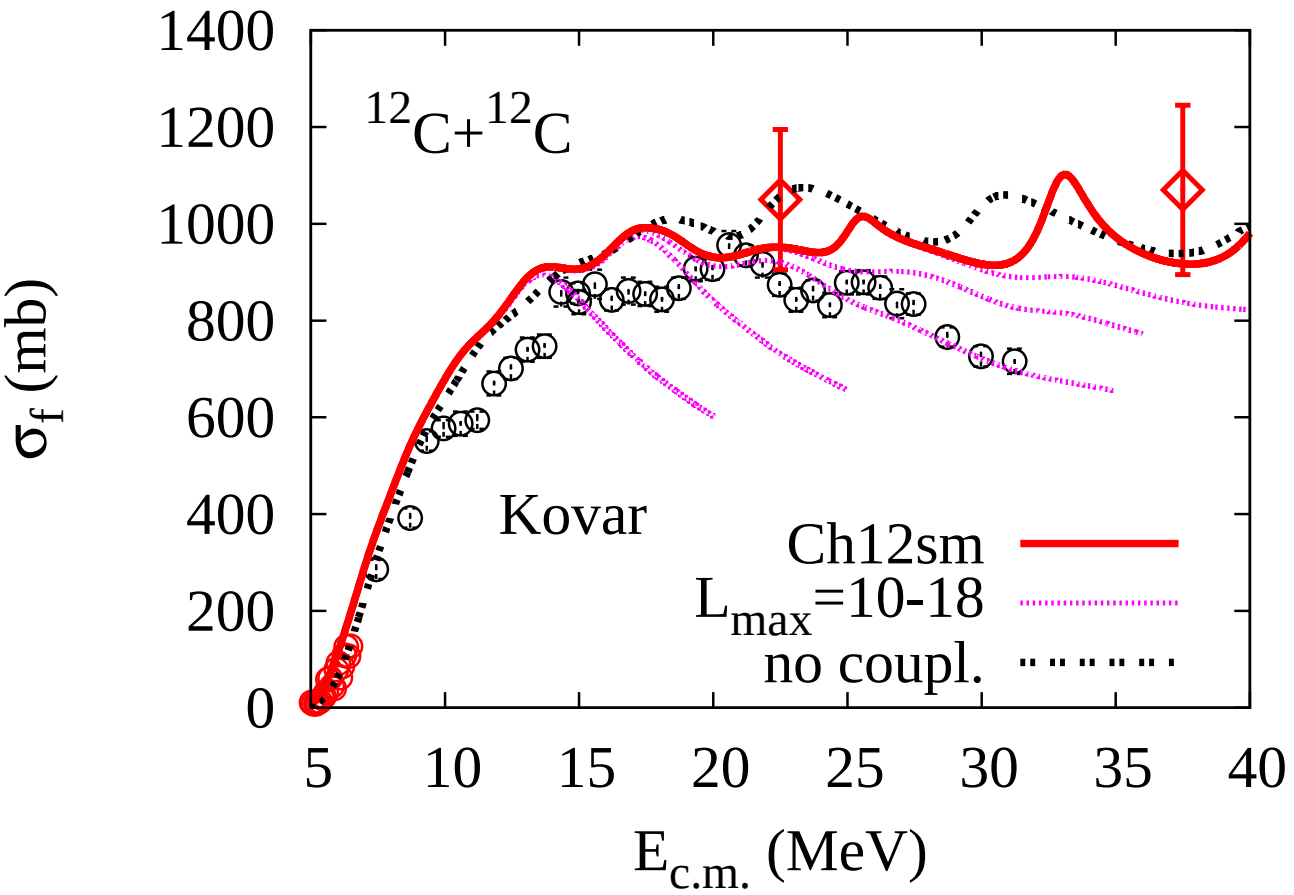

The data were recently confirmed by Rehm et al. (MUSIC). Vandenbosch, PLB 87, 183 (1979), explained the suppression by the low level density of I=8, 10, 12 .. states in ^{24}Mg.

Effective centrifugal barriers in ^{12}C+^{12} fusion

are revealed in a $d(E\sigma_f)/dE$ plot.